

See discussions, stats, and author profiles for this publication at: <https://www.researchgate.net/publication/231659189>

# Effect of the Substrate Morphology on the Structure of Adsorbed Ice

ARTICLE *in* THE JOURNAL OF PHYSICAL CHEMISTRY B · JUNE 1997

Impact Factor: 3.3 · DOI: 10.1021/jp9702412

---

CITATIONS

25

---

READS

22

## 3 AUTHORS:



[Sofia Trakhtenberg](#)

Warner Babcock Institute

**28** PUBLICATIONS **553** CITATIONS

[SEE PROFILE](#)



[Ron Naaman](#)

Weizmann Institute of Science

**304** PUBLICATIONS **5,354** CITATIONS

[SEE PROFILE](#)



[Sidney R Cohen](#)

Weizmann Institute of Science

**175** PUBLICATIONS **4,874** CITATIONS

[SEE PROFILE](#)

# Effect of the Substrate Morphology on the Structure of Adsorbed Ice

S. Trakhtenberg,<sup>†</sup> R. Naaman,<sup>\*,†</sup> and S. R. Cohen<sup>‡</sup>

Department of Chemical Physics, and Chemical Services, Weizmann Institute of Science, Rehovot 76100, Israel

I. Benjamin

Department of Chemistry, University of California, Santa Cruz, California 95064

Received: January 16, 1997; In Final Form: April 15, 1997<sup>®</sup>

New observations on the effect of surface morphology (corrugation) on the structure of vapor-deposited ice are presented. Amorphous quartz and single-crystal Si(100) were used as substrates. Water was deposited on the bare substrates and on the substrates covered with organized organic thin films (OOTF). By coating the substrates with mixed organic monolayers, controlled corrugation was achieved, without affecting the chemical nature of the surface. Information on the surface corrugation on different scales was obtained by atomic force microscopy and wettability measurement techniques. The ice phase was determined by *in situ* infrared absorption measurements. Correlation was observed between the surface roughness on a scale that is characteristic for the distance between ice nucleation centers and the deposited ice structure. Molecular dynamics simulations could reproduce the experimental observations and provide an insight into its origin.

## Introduction

The investigation of the structure of ice has been the subject of a large number of studies due to its obvious importance to many areas in science. In astrophysics,<sup>1–3</sup> cometary nuclei are thought to be formed of partially crystallized amorphous ice.<sup>4</sup> Amorphous ice is used in cryobiology<sup>5</sup> as a model for liquid water at low temperatures. Systematic investigations of the amorphous ice have been instrumental for better understanding of the properties of liquid water.<sup>6</sup> In addition, water ice plays an important role in atmospheric chemistry, since part of polar stratospheric clouds consist of small ice particles.<sup>7–9</sup>

Here, we present new evidence on the effect of substrate morphology (corrugation) on the structure of the vapor-deposited ice. Organized organic layers were applied in order to modify the surface corrugation without altering its chemical nature.

In past studies it has been found that the phase of the ice may affect the chemistry of molecules adsorbed on its surface.<sup>10</sup> Therefore, it is important to understand how the ice properties depend on the substrate on which the ice is formed. For example, in comets<sup>11</sup> and interstellar dense clouds,<sup>12</sup> ice is adsorbed on dust. These dust particles are made from silicates. A convenient way to study the thermal history of comets is to monitor the kinetics of the slow crystallization of the amorphous ice component.<sup>4</sup> However, the interaction between the dust substrate and the ice are usually neglected in these studies. Different substrates were used for studying vapor-deposited amorphous ices. Most common substrates were metals, such as Cu<sup>13</sup> and Al,<sup>2</sup> ionic compounds such as KBr,<sup>14</sup> and amorphous substrates such as carbon.<sup>1</sup> Ice deposition was also performed on more exotic substrates such as organized organic films with both hydrophobic and hydrophilic nature.<sup>15</sup> Nevertheless, the influence of substrate on the structure of the deposited ice remains in many of these experiments an undefined parameter. However in recent work surprising results were reported.<sup>16</sup> Water ice is known to have an amorphous structure when deposited on a solid substrate such as Al at temperatures below

50 K. However ice adsorbed at  $T < 20$  K on oxygen-deficient highly porous silicate smokes formed a crystalline phase. This substrate is highly relevant to astrophysics. These results may be crucial for understanding the thermal history of the universe.

The substrate effect on the desorption kinetics of vapor-deposited amorphous ice was investigated for hydrophobic Au(111) and hydrophilic Ru(001) single-crystal substrates.<sup>17</sup> The desorption kinetics was found to be substrate dependent. Nevertheless, no difference between the crystallization kinetics of the two amorphous deposits was observed.

The effect of substrate roughness on ice desorption temperature was measured for Pt, Pd, Ni, and Cu single-crystal substrates. It was found that ice desorbed from rougher (110) surfaces at significantly higher temperatures than from smoother (100) and (111) surfaces.<sup>18</sup>

The effect of the surface on ice crystallization was also investigated for ice nucleation under regular and mixed monolayers of aliphatic alcohols.<sup>19</sup> The freezing temperatures of water covered by mixed monolayers were found to be lower than the freezing points obtained for each of the pure monolayers. It was proposed that this effect results from surface roughness at the monolayer–water interface.

Here, in addition to the new experimental results, based on molecular dynamic simulations, a model is presented to explain the effect of morphology on the ice phase.

## Experimental Section

The experiments were performed in an ultrahigh-vacuum chamber which is inserted into the measuring compartment of a FTIR spectrometer (Bruker IFS 66) allowing *in situ* direct infrared absorption measurements. Water vapors were introduced into the chamber through a stainless steel tube. The sample temperature could be controlled between 90 and 500 K with an accuracy of one degree.

Various substrates were used in the present study: quartz (amorphous), single-crystal silicon (100) wafer, quartz and silicon covered with organized monolayers of octadecyltrichlorosilane [OTS = CH<sub>3</sub>(CH<sub>2</sub>)<sub>17</sub>SiCl<sub>3</sub>], and both substrates covered with mixed organized monolayers, where the mixtures contain OTS and docosyltrichlorosilane [DTS = CH<sub>3</sub>(CH<sub>2</sub>)<sub>21</sub>SiCl<sub>3</sub>] in

<sup>†</sup> Department of Chemical Physics.

<sup>‡</sup> Chemical Services.

<sup>®</sup> Abstract published in *Advance ACS Abstracts*, June 15, 1997.

**TABLE 1: Results on the Adsorbed Ice Phase and the Surface Morphology**

film and substrate	ice structure and its dependence on deposition rate	desorption temperature	contact angle		rms roughness (nm)		surface fractal dimension
			H <sub>2</sub> O	BCH	few nm range <sup>a</sup>	whole range	
quartz	more crystalline as deposition rate increases	141 ± 5 K			0.03 ± 0.01 0.07 ± 0.01 0.18 ± 0.05	0.75 ± 0.15	2.34 ± 0.05
OTS on quartz	more crystalline as deposition rate increases	146 ± 5 K	112°	48°	0.03 ± 0.01 0.05 ± 0.01 0.15 ± 0.05	0.65 ± 0.15	2.30 ± 0.05
OTS–DTS (1:1) on quartz	amorphous independent of deposition rate	153 ± 5 K	113°	40°	0.06 ± 0.01 0.09 ± 0.01 0.22 ± 0.05	0.70 ± 0.15	2.46 ± 0.04
OTS–DTS (4:1) on quartz	amorphous independent of deposition rate	155 ± 4 K	112°	41°			
OTS–DTS (9:1) on quartz	amorphous independent of deposition rate	158 ± 5 K	112°	43°			
silicon wafer	amorphous independent of deposition rate	169 ± 3 K			0.12 ± 0.02 0.22 ± 0.05 0.4 ± 0.1	1.6 ± 0.4	2.47 ± 0.06
OTS on silicon wafer	amorphous independent of deposition rate	170 ± 3 K	113°	49°	0.06 ± 0.015 0.09 ± 0.02 0.20 ± 0.05	0.85 ± 0.1	2.43 ± 0.04
OTS–DTS (1:1) on silicon wafer	more crystalline as deposition rate increases	≈100 K	112°	42°	0.03 ± 0.01 0.045 ± 0.015 0.13 ± 0.02	0.65 ± 0.1	2.35 ± 0.03

<sup>a</sup> The numbers correspond to 5–10, 5–20, and 10–50 nm ranges, respectively.

1:1 proportion. In addition, quartz slides covered with mixed OTS–DTS monolayers in 4:1 and 9:1 proportions were used. The monolayers were prepared using the self-assembly technique.<sup>20</sup> In order to ensure the monolayers' quality, wettability measurements were performed.

The samples were cooled to 100 K and exposed to the water vapor. Deposition rate was varied between  $3 \times 10^{-3}$  to  $8 \times 10^{-2}$   $\mu\text{m/h}$ . After deposition of the desired amount of ice, the substrate temperature was raised at a rate of 0.75 K/min. The changes in the infrared absorption of the deposited ice were monitored.

The morphology of the substrates was measured by an atomic force microscope (Topometrix TMX 2010 Discoverer AFM). Intermittent contact mode imaging was used with an integrated Si cantilever/tip (Nanoprobe) with a resonance frequency between 280 and 320 kHz. Tips were changed frequently as needed when degradation of image sharpness was observed. We obtained several pictures of area 500 nm  $\times$  500 nm for each substrate. Larger or smaller fields of view did not have the resolution or the frequency range necessary for the analysis. The roughness values given represent the average over three pictures. Several criteria were checked for surface roughness. First, average roughness (root mean square, rms) and fractal dimension were calculated. Then, using the power spectral density analysis available on the Topometrix SPMLAB analysis software, the integrated roughness over specific distance scales was calculated. Power spectral density plots display the "roughness power" as a function of frequency. The units of the ordinate are given in  $\text{nm}^2 \mu\text{m}^{-1}$ . Integrating this function over the desired spectral range gives the roughness power within this range, and the square root of this integral yields the rms values displayed in Table 1. We chose the scales that seem to be relevant to the distances between ice nucleation centers: 5–10, 5–20, and 10–50 nm.

The IR absorption spectrum of ice provides information on its phase.<sup>14</sup> Two forms of ice could be distinguished by their FTIR spectra: an amorphous form, which is characterized by a peak at about 3250  $\text{cm}^{-1}$  with a shoulder at about 3400  $\text{cm}^{-1}$ , and a partially crystalline form, which exhibits an absorption peak at about 3230  $\text{cm}^{-1}$  with two shoulders at about 3150 and

3350  $\text{cm}^{-1}$ . The absorption spectra were analyzed by taking the first derivatives of the absorption spectra. The resulting plots are very sensitive to changes in the spectra and show clearly the differences between the amorphous and crystalline ice.

## Results and Discussion

The degree of crystallinity of the adsorbate is known to depend on the deposition rate.<sup>21</sup> In the range of adsorption rate investigated, no effect of deposition rate was found for the silicon substrate. Yet, the shape of the IR absorption band did depend on the deposition rate for water deposited on the quartz substrate. When the deposition rate was high, structures with a large fraction of crystalline ice were obtained (Figure 1A). At low deposition rates the ice crystallinity is less pronounced (Figure 1B). The structure of ice deposited on silicon wafer was found to be amorphous (Figure 1C). The differences between the spectra of amorphous and partially crystalline ice are even more pronounced when they are presented as the first-order derivatives of the absorption peaks (Figure 1A',B',C').

Figure 2 shows the spectra of  $(1.6 \pm 0.1) \times 10^{-3}$   $\mu\text{m}$  (about five layers<sup>22</sup>) of ice adsorbed on different substrates. The deposition rate was  $3 \times 10^{-3}$   $\mu\text{m/h}$ . The absorption bands of ice deposited both on quartz (Figure 2A) and on quartz covered with an OTS monolayer (Figure 2B) have two well-pronounced shoulders each. This spectrum is an indication of the partially crystalline structure of the ice. On the other hand, the absorption bands of ice deposited on a silicon wafer (Figure 2C) and on silicon wafers covered with an OTS monolayer (Figure 2D) correspond to the amorphous phase.

In order to check the origin of the substrate effect and to understand why the organized organic film does not alter the phase of the ice, the substrates were covered with mixed organized organic monolayers. It is important to realize that the chemical nature of the terminal groups, in both the pure and mixed type monolayers, is identical; namely, it is the methyl ( $-\text{CH}_3$ ) group. Figure 3 presents, for comparison, the spectrum of ice deposited at 100 K on each of the four substrates: quartz

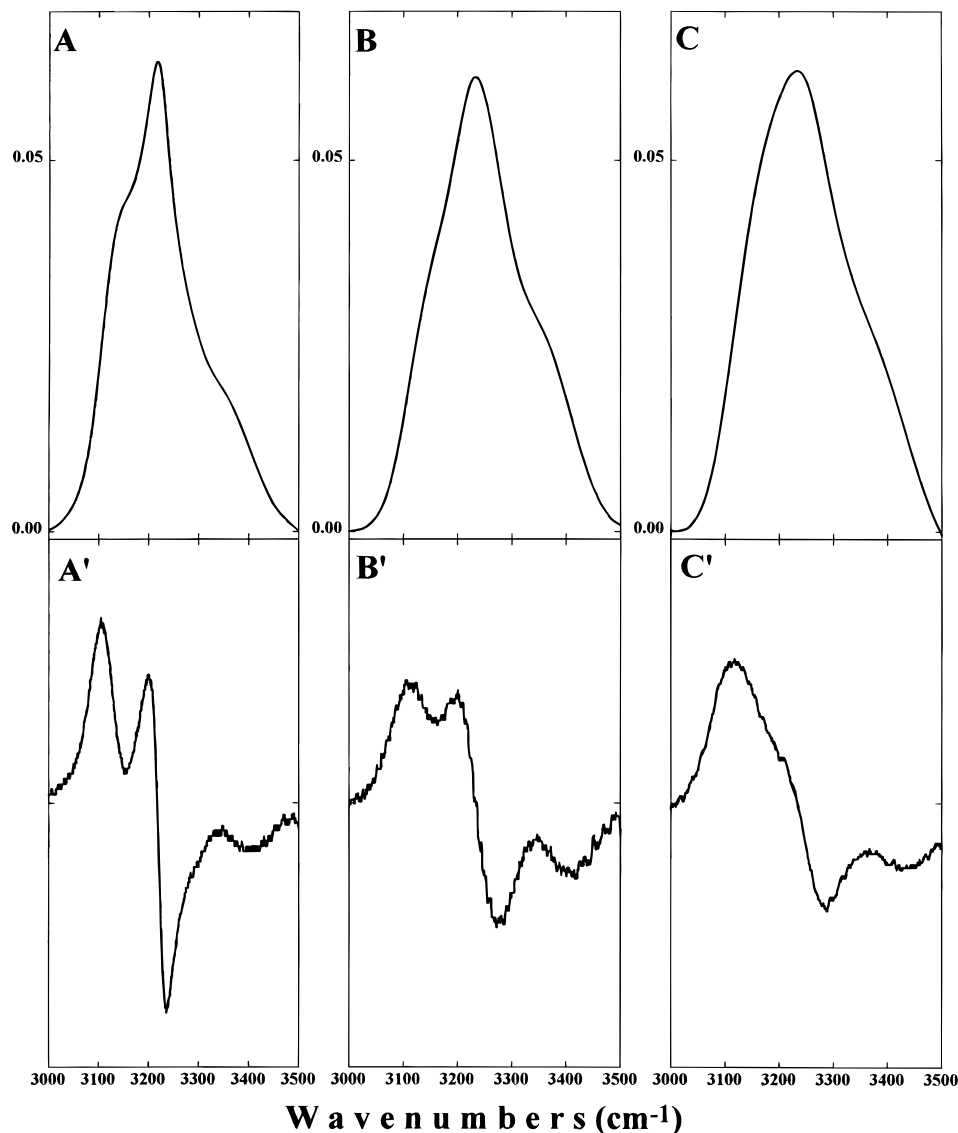


**Figure 1.** FTIR absorbance spectra of water deposited at 100 K on a quartz slide with a deposition rate of  $5 \times 10^{-2} \mu\text{m/h}$  (A), on a quartz slide with a deposition rate of  $2 \times 10^{-3} \mu\text{m/h}$  (B), and on a Si wafer with a deposition rate of  $5 \times 10^{-2} \mu\text{m/h}$  (C). Underneath each spectrum its first-order derivative is presented in parts A', B', and C', respectively.

coated with OTS (A); silicon covered with OTS (B); quartz coated with a mixed OTS–DTS (1:1) monolayer (C); and silicon coated with the mixed monolayer (D). It can clearly be seen that the spectrum of ice adsorbed on the mixed monolayer adsorbed on quartz is very similar to that of ice adsorbed on OTS-coated silicon, while the ice on OTS-coated quartz has more crystalline characteristics and is similar to the ice adsorbed on the mixed monolayer on top of the silicon wafer. Spectra of ice samples deposited on other mixed monolayers (4:1 and 9:1) are similar to the one in which the ratio was 1:1.

Strong indication of the nature of the ice phase is provided by the temperature dependent measurements. Water layers of thickness  $3.5 \times 10^{-3} \mu\text{m}$  were deposited at 100 K on various substrates and heated at a rate of 0.75 K/min. Figure 4 presents the intensity of the infrared absorption water band as a function of surface temperature. As the temperature increases, the intensity decreases due to water desorption. From quartz substrates, both clean and covered with OTS, water desorbed at about 140 K. Water deposited on silicon substrates, both clean and covered with OTS, desorbed at about 170 K. Desorption of water from quartz substrates covered with the mixed OTS–DTS monolayers occurs at an intermediate temperature. Desorption of water from silicon substrates covered

with the mixed OTS–DTS monolayers occurs at a temperature just above 100 K and is not presented in the figure.

For all surfaces studied, no correlation could be observed between the ice phase and the contact angles measured with water and bicyclohexyl (BCH). However, surface roughness, as determined by AFM, demonstrates clear correlation between corrugation at a specific scale and the ice phase. As expected, it was found that the definition of “smooth” and “rough” depends on the exact scale. Table 1 presents the results obtained on different scales, by contact angle and AFM measurements, for all the surfaces.

The rms averaged roughness of the surfaces that is extracted from the AFM studies also does not show significant differences between the samples. However on the scale of a few nanometers the silicon and silicon coated with OTS were found to be the rougher surfaces, while the quartz and quartz coated with OTS are the smoother ones. Coating the surface with OTS decreases its roughness. When the quartz is coated with the mixed monolayer, its roughness on the given scale increased, while when the Si wafer is covered with a mixed monolayer, its roughness decreased. This is probably due to the fact that the long organic chains tend to adsorb on the low areas, while the short ones are adsorbed on the higher parts of the surface.

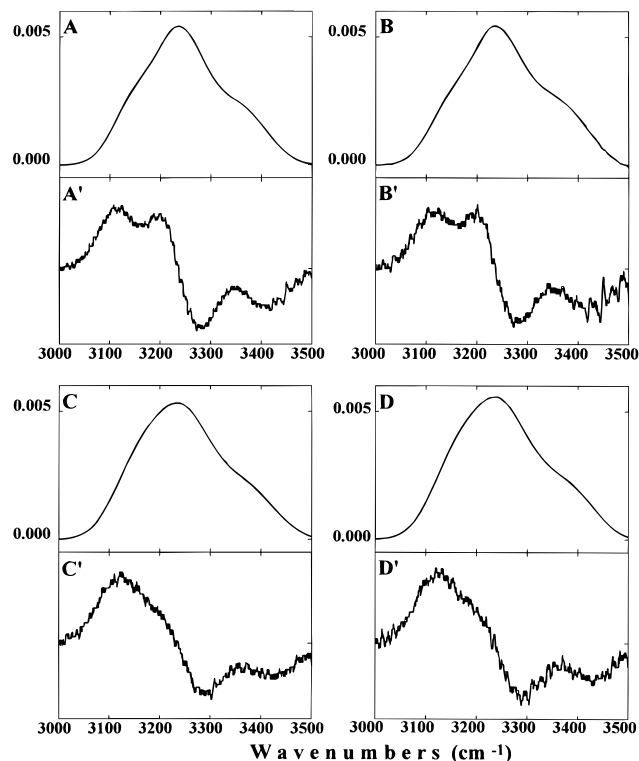


**Figure 2.** FTIR absorbance spectra of 0.001  $\mu\text{m}$  of water deposited at 100 K on (A) quartz; (B) quartz covered with OTS; (C) silicon; and (D) silicon covered with OTS. The first-order derivatives of spectra are presented in parts A', B', C', and D', respectively.

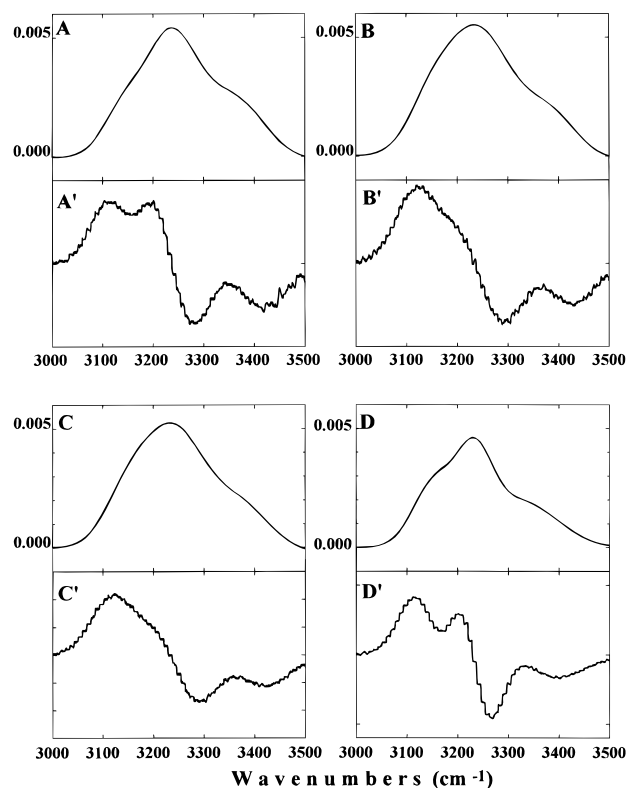


**Figure 3.** FTIR absorbance spectra of water deposited at 100 K on quartz coated with OTS (A), on silicon coated with OTS (B), on quartz covered with a mixed OTS-DTS monolayer (C), and on quartz covered with a mixed OTS-DTS monolayer (9:1) (D). The first order derivatives of spectra are presented in parts A', B', C', and D', respectively.

This adsorption pattern minimizes the free energy of the monolayer and decreases the roughness.

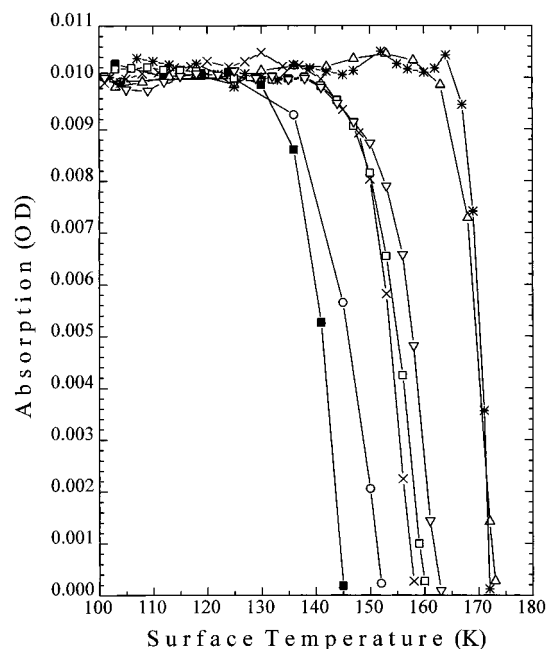


**Figure 4.** Temperature dependence of the IR absorbance for water deposited on (■) quartz, (○) quartz covered with OTS, (△) silicon wafer, (\*) silicon covered with OTS, (×) quartz covered with a mixed OTS-DTS (1:1) monolayer, (□) quartz covered with a mixed OTS-DTS (4:1) monolayer, (▽) quartz covered with a mixed OTS-DTS (9:1) monolayer.

**TABLE 2: Parameters Used in the Molecular Dynamics Simulation**

substrate area	25 nm <sup>2</sup>
number of peaks on the substrate	4
peak height	0.4 nm
number of molecules	50
water-water potential	see ref 24
water-substrate potential	$-2.3 \text{ kcal/mol} \times ((0.23 \text{ nm}/r)^3 - (0.23 \text{ nm}/r)^9)$
equilibration time	200 ps
run time	45 ps

In order to gain insight into the relation between the surface morphology and the ice phase, molecular dynamics simulations were performed<sup>23</sup> on a system of 50 water molecules interacting with a wall of surface area  $5 \times 5 \text{ nm}$  (this corresponds to a submonolayer of water). The water-water potential was described using the simple point charge model.<sup>24</sup> The water-wall interactions were taken to be a 3-9 Lennard-Jones in the direction perpendicular to the surface and periodic in the plane parallel to the surface. In this model, corrugation is simply introduced via the parameters that control the number of peaks (the periodicity of the lattice) and their height. In particular, by varying the number of peaks, one can produce a substrate that can either support or inhibit the formation of an icelike structure. After an equilibration period at 100 K, statistics were collected for several choices of surface roughness. The parameters used in the simulation are shown in Table 2.

In the simulation it was found that if the number of peaks, for the given area, was greater than four, the results for the smooth and rough surface were identical. If the number of peaks was two, again no effect could be observed. However in the case of four peaks, the effect of surface roughness was pronounced. The results are presented in Figure 5, where the oxygen-oxygen radial (three-dimensional) distribution function (normalized by the density of bulk water) is plotted for the rough and smooth surfaces. The first maxima of both distributions (on smooth and rough surfaces) are at the same oxygen-oxygen

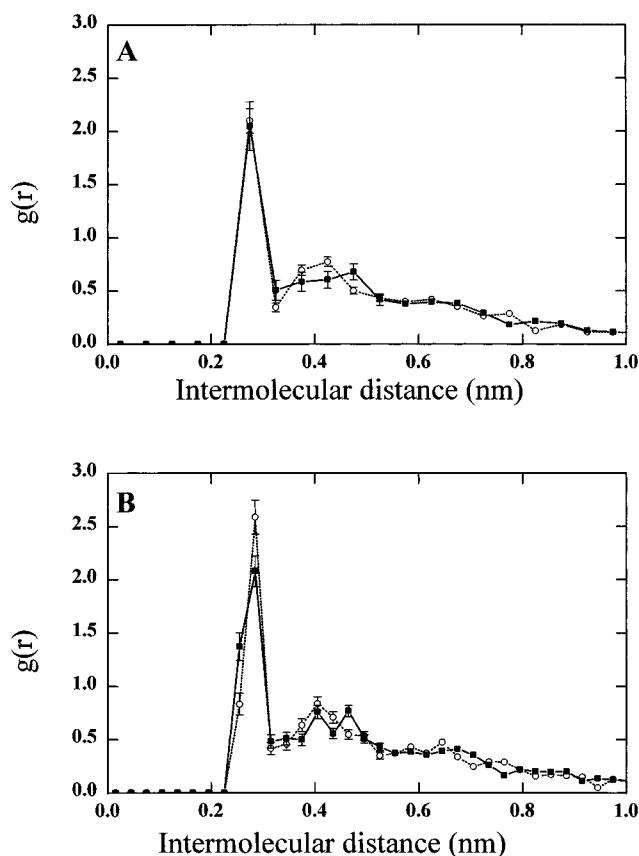


**Figure 5.** Ice radial distribution function,  $g(r)$ , calculated for 50  $\text{H}_2\text{O}$  molecules deposited on a (—■—) smooth surface and on a (···○···) rough surface. (A) Resolution is 0.05 nm. (B) Resolution is 0.03 nm.

distance, at about 0.275 nm. This value is in good agreement with X-ray diffraction of crystalline ice.<sup>25,26</sup> In crystalline ice, the next maxima are at about 0.45 and 0.47 nm. We found that in the simulation there are maxima at about 0.41 nm for the rough substrate and 0.47 nm for the smooth substrate. If the density function is presented at higher resolution, then for the smooth substrate we observe a double maximum at 0.41 and 0.46 nm, respectively. The first maximum corresponds to the same maximum observed on the rough substrate, and the second one fits the expected value for crystalline ice. Hence, we conclude that on the simulated “rough” substrate, amorphous ice grows, while on the “smooth” substrate a mixture of amorphous and crystalline ice is formed.

The mean distance between nucleation embryos in amorphous vapor-deposited ice was found to be about 5 nm.<sup>17</sup> Using this distance scale as the relevant one for the present study, we note the excellent correlation between surface roughness at the sub 20 nm scale and the preferred crystallization type. This correlation weakens for the 10–50 nm scale and disappears completely when roughness of the entire  $500 \times 500$  nm picture is considered. This comparison emphasizes the importance of using power spectral density analysis to isolate the relevant roughness scale. The surface fractal dimension analysis, as presented in Table 1, confirms this correlation of roughness with crystallization type. Although the fractal dimension is less rigorously correlated with surface roughness on a particular scale, larger values indicate more roughness at smaller scales. Hence, in this case quartz (and quartz coated with OTS) is the smoother surface, while Si (and Si coated with OTS) is the rougher one. The experimental found relevant length is in agreement with the corrugation scale found to be effective in the simulation.

The question remains, why is the ice formed on a smooth surface more crystalline than that formed on the corrugated surfaces?

On smooth surfaces, the average interaction between the adsorbed molecule and the surface is weaker than on the rough one. This is due to the fact that if the roughness is on the dimension of a few molecules, the adsorbates (either the single molecules or the whole cluster) interact with several sites on the surface simultaneously. On the other hand, on the smooth surface the interaction is only with a single site. Therefore on the smooth surface the water molecules distribute more evenly. As a result, on the smooth surface, the adsorbed water molecules are more free to move and can arrange themselves in the most stable configuration. Due to the relatively weak adsorbate–surface interaction, in the case of smooth surfaces, the adsorbate desorbs from the surface at lower temperature. The above description is consistent with our observations. The ice adsorbed on quartz and on quartz covered with OTS is more crystalline and desorbs at a lower temperature than ice adsorbed on silicon, silicon covered with OTS, and quartz covered with the mixed monolayer (Figures 2, 3, and 4).

The results presented here indicate that the substrate morphology may play an important role in defining the ice state. In addition, it demonstrates that the surfaces of organized organic films of silanes project the morphology of the underlying substrate.

## References and Notes

- (1) Jenniskens, P.; Blake, D. E. *Science* **1994**, 265, 753.
- (2) Moore, M. H.; Hudson, R. L. *Astrophysical J.* **1992**, 401, 353; *J. Phys. Chem.* **1992**, 96, 6500.
- (3) Mayer, E.; Pletzer, R. *Nature* **1986**, 319, 298.
- (4) Tancredy, G.; Rickman, H.; Greenberg, G. M. *Astron. Astrophys.* **1994**, 286, 659.
- (5) Mazur, P. *Science* **1970**, 168, 939.
- (6) Sceats, M. G.; Rice, S. A. In *Water: A Comprehensive Treatise*; Franks, F., Ed.; Plenum: New York, 1982; Vol. 7, pp 83–214.
- (7) Horn, A. B.; Chesters, M. A.; McCoustra, M. R. S.; Sodeau, J. R. *J. Chem. Soc., Faraday Trans.* **1992**, 88, 1077; *J. Phys. Chem.* **1994**, 98, 946.
- (8) Tolbert, M. A.; Rossi, M. J.; Golden, D. M. *Science* **1988**, 240, 1018.
- (9) Clary, D. C. *Science*, **1996**, 271, 1509.
- (10) Gertner, B. J.; Hynes, J. T. *Science* **1996**, 271, 1563.
- (11) Bregman, J. D.; Campins, H.; Witteborn, F. C.; Wooden, D. H.; Rank, D. M.; Allamandola, L. J.; Cohen, M.; Tielens, A. G. G. M. *Astron. Astrophys.* **1987**, 187, 616.
- (12) Nuth, J. A., III; Hecht, J. H. *Astrophys. Space Sci.* **1990**, 163, 79.
- (13) Hallbrucker, A.; Mayer, E.; Johari, G. P. *J. Phys. Chem.* **1989**, 93, 4986.
- (14) Bergen, M. S.; Schuh, D.; Sceats, M. G.; Rice, S. A.; *J. Chem. Phys.* **1978**, 69, 3477.
- (15) Nuzzo, R. G.; Zegarski, B. R.; Korenic, E. M.; Dubois, L. H. *J. Phys. Chem.* **1992**, 96, 1355.
- (16) Moore, M. H.; Ferrante, R. F.; Hudson, R. L.; Nuth, J. A., III; Donn, B. *Astrophys. J.* **1994**, 428 L81.
- (17) Smith, R. S.; Huang, C.; Wong, E. K. L.; Kay, B. D. *Surf. Sci.* **1996**, 367, L13.
- (18) Thiel, P. A.; Madey, T. E. *Surf. Sci. Rep.* **1987**, 7, 211.
- (19) Popovitz-Biro, R.; Wang, J. L.; Majewski, J.; Shavit, E.; Leiserowitz, L.; Lahav, M. *J. Am. Chem. Soc.* **1994**, 116, 1179.
- (20) Sagiv, J. *J. Am. Chem. Soc.* **1980**, 102, 92.
- (21) Olander, D. S.; Rice, S. A. *Proc. Natl. Acad. Sci. U.S.A.* **1972**, 69, 98.
- (22) Bertie, J. E.; Labbe, H. J.; Whalley, E. *J. Chem. Phys.* **1969**, 50, 4501.
- (23) Benjamin, I. *Chem. Rev.* **1996**, 96, 1449.
- (24) Berendsen, H. J. C.; Postma, J. P. M.; van Gunsteren, W. F.; Hermans, J. In *Intermolecular Forces*; Pullman, B., Ed.; Reidel: Dordrecht 1981.
- (25) (a) Lonsdal, K. *Proc. R. Soc.* **1958**, A247, 424. (b) Brill, R.; Tippe, A. *Acta Crystallogr.* **1967**, 23, 343.
- (26) *Structural Chemistry and Molecular Biology*; Rich, A.; Davidson, N., Eds.; W. H. Freeman and Co. New York, 1968; p 507.